

ISO 25498:2018

MARS 2018

www.afnor.org

Ce document est à usage exclusif et non collectif des clients AFNOR.
Toute mise en réseau, reproduction et rediffusion, sous quelque forme que ce soit, même partielle, sont strictement interdites.

This document is intended for the exclusive and non collective use of AFNOR customers.
All network exploitation, reproduction and re-dissemination, even partial, whatever the form (hardcopy or other media), is strictly prohibited.



**DOCUMENT PROTÉGÉ
PAR LE DROIT D'AUTEUR**

Droits de reproduction réservés. Sauf prescription différente, aucune partie de cette publication ne peut être reproduite ni utilisée sous quelque forme que ce soit et par aucun procédé, électronique ou mécanique, y compris la photocopie et les microfilms, sans accord formel.

Contacteur :
AFNOR – Norm'Info
11, rue Francis de Pressensé
93571 La Plaine Saint-Denis Cedex
Tél : 01 41 62 76 44
Fax : 01 49 17 92 02
E-mail : norminfo@afnor.org

afnor

AFNOR

Pour : GN-MEBA

Client : 23432617

le : 12/04/2018 à 16:59

Diffusé avec l'autorisation de l'éditeur

Distributed under licence of the publisher

INTERNATIONAL STANDARD

ISO 25498

Second edition
2018-03

Microbeam analysis — Analytical electron microscopy — Selected area electron diffraction analysis using a transmission electron microscope

*Analyse par microfaisceaux — Microscopie électronique analytique
— Analyse par diffraction par sélection d'aire au moyen d'un
microscope électronique en transmission*



Reference number
ISO 25498:2018(E)

© ISO 2018

ISO 25498:2018(E)



COPYRIGHT PROTECTED DOCUMENT

© ISO 2018

All rights reserved. Unless otherwise specified, or required in the context of its implementation, no part of this publication may be reproduced or utilized otherwise in any form or by any means, electronic or mechanical, including photocopying, or posting on the internet or an intranet, without prior written permission. Permission can be requested from either ISO at the address below or ISO's member body in the country of the requester.

ISO copyright office
CP 401 • Ch. de Blandonnet 8
CH-1214 Vernier, Geneva
Phone: +41 22 749 01 11
Fax: +41 22 749 09 47
Email: copyright@iso.org
Website: www.iso.org

Published in Switzerland

Contents

	Page
Foreword.....	iv
Introduction.....	vi
1 Scope.....	1
2 Normative references.....	1
3 Terms and definitions.....	1
4 Principle.....	3
4.1 General.....	3
4.2 Spot diffraction pattern.....	3
4.3 Kikuchi pattern.....	6
4.4 Polycrystalline specimen.....	7
5 Reference materials.....	7
6 Equipment.....	8
7 Specimens.....	8
8 Experimental procedure.....	8
8.1 Instrument preparation.....	8
8.2 Procedure for acquirement of selected area electron diffraction patterns.....	9
8.3 Determination of diffraction constant, $L\lambda$	12
9 Measurement and solution of the SAED patterns.....	13
9.1 Selection of the basic parallelogram.....	13
9.2 Indexing diffraction spots.....	15
10 180° ambiguity.....	16
11 Uncertainty estimation.....	16
11.1 Factors affecting accuracy.....	16
11.2 Calibration with a reference material.....	17
Annex A (informative) Interplanar spacing.....	18
Annex B (informative) Spot diffraction patterns of single crystals for BCC, FCC and HCP structure[7].....	19
Bibliography.....	38

ISO 25498:2018(E)

Foreword

ISO (the International Organization for Standardization) is a worldwide federation of national standards bodies (ISO member bodies). The work of preparing International Standards is normally carried out through ISO technical committees. Each member body interested in a subject for which a technical committee has been established has the right to be represented on that committee. International organizations, governmental and non-governmental, in liaison with ISO, also take part in the work. ISO collaborates closely with the International Electrotechnical Commission (IEC) on all matters of electrotechnical standardization.

The procedures used to develop this document and those intended for its further maintenance are described in the ISO/IEC Directives, Part 1. In particular the different approval criteria needed for the different types of ISO documents should be noted. This document was drafted in accordance with the editorial rules of the ISO/IEC Directives, Part 2 (see www.iso.org/directives).

Attention is drawn to the possibility that some of the elements of this document may be the subject of patent rights. ISO shall not be held responsible for identifying any or all such patent rights. Details of any patent rights identified during the development of the document will be in the Introduction and/or on the ISO list of patent declarations received (see www.iso.org/patents).

Any trade name used in this document is information given for the convenience of users and does not constitute an endorsement.

For an explanation on the voluntary nature of standards, the meaning of ISO specific terms and expressions related to conformity assessment, as well as information about ISO's adherence to the World Trade Organization (WTO) principles in the Technical Barriers to Trade (TBT) see the following URL: www.iso.org/iso/foreword.html.

This document was prepared by Technical Committee ISO/TC 202, *Microbeam analysis*, Subcommittee SC 3, *Analytical electron microscopy*.

This second edition cancels and replaces the first edition (ISO 25498:2010), which has been technically revised.

The main changes to the previous edition are as follows:

- the foreword has been revised;
- the introduction has been revised;
- the scope has been revised;
- the figure of Ewald construction has been deleted;
- the terms and definition of terminological entries [3.1](#), [3.2](#), [3.10](#), [3.11](#), [3.12](#), [3.13](#) and [3.14](#) have been added;
- the subclause [4.1](#) has been added;
- [Clause 5](#) has been revised;
- [Clauses 4](#), [6](#), [7](#), and [10](#) and subclauses [8.1.5](#), [8.1.6](#), [8.2.1](#), [8.2.2](#), [8.2.4](#), [8.2.7](#), [8.2.8](#), [8.2.11](#) and [9.1.2](#) have been editorially revised;
- the subclause [9.2.5](#) has been added;
- all formulae have been renumbered;
- [Annex A](#) has been revised;
- the subclause [B.1](#) has been revised;

ISO 25498:2018(E)

- the figures have been modified;
- the bibliography has been updated.

ISO 25498:2018(E)

Introduction

Electron diffraction techniques are widely used in transmission electron microscopy (TEM) studies. Applications include phase identification, determination of the crystallographic lattice type and lattice parameters, crystal orientation and the orientation relationship between two phases, phase transformations, habit planes and defects, twins and interfaces, as well as studies of preferred crystal orientations (texture). While several complementary techniques have been developed, for example microdiffraction, convergent beam diffraction and reflected diffraction, the selected area electron diffraction (SAED) technique is the most frequently employed.

This technique allows direct analysis of small areas on thin specimens from a variety of crystalline substances. It is routinely performed on most of TEM in the world. The SAED is also a supplementary technique for acquisition of high resolution images, microdiffraction or convergent beam diffraction studies. The information generated is widely applied in the studies for the development of new materials, improving structure and/or properties of various materials as well as for inspection and quality control purpose.

The basic principle of the SAED method is described in this document. The experimental procedure for the acquirement of SAED patterns, indexing of the diffraction patterns and determination of the diffraction constant are specified. ISO 25498 is intended for use or reference as technical regulation for transmission electron microscopy.

Microbeam analysis — Analytical electron microscopy — Selected area electron diffraction analysis using a transmission electron microscope

1 Scope

This document specifies the method of selected area electron diffraction (SAED) analysis using a transmission electron microscope (TEM) to analyse thin crystalline specimens. This document applies to test areas of micrometres and sub-micrometres in size. The minimum diameter of the selected area in a specimen which can be analysed by this method is restricted by the spherical aberration coefficient of the objective lens of the microscope and approaches several hundred nanometres for a modern TEM.

When the size of an analysed specimen area is smaller than that restriction, this document can also be used for the analysis procedure. But, because of the effect of spherical aberration, some of the diffraction information in the pattern can be generated from outside of the area defined by the selected area aperture. In such cases, the use of microdiffraction (nano-beam diffraction) or convergent beam electron diffraction, where available, might be preferred.

This document is applicable to the acquisition of SAED patterns from crystalline specimens, indexing the patterns and calibration of the diffraction constant.

2 Normative references

The following documents are referred to in the text in such a way that some or all of their content constitutes requirements of this document. For dated references, only the edition cited applies. For undated references, the latest edition of the referenced document (including any amendments) applies.

ISO/IEC 17025, *General requirements for the competence of testing and calibration laboratories*

3 Terms and definitions

For the purposes of this document, the following terms and definitions apply.

ISO and IEC maintain terminological databases for use in standardization at the following addresses:

- ISO Online browsing platform: available at <https://www.iso.org/obp>
- IEC Electropedia: available at <http://www.electropedia.org/>

3.1

Miller index

notation system for crystallographic planes and directions in crystals, in which a set of lattice planes or directions is described by three axes coordinate

3.2

Miller-Bravais index

notation system for crystallographic planes and directions in hexagonal crystals, in which a set of lattice planes or directions is described by four axes coordinate

3.3

$(h\ k\ l)$

Miller indices (3.1) of a specific set of crystallographic planes

ISO 25498:2018(E)

3.4

$\{hkl\}$

Miller indices (3.1) which denote a family of crystallographic planes

3.5

$[uvw]$

Miller indices (3.1) of a specific crystallographic direction or a zone axis

3.6

interplanar spacing

d_{hkl}

perpendicular distance between consecutive planes of the crystallographic plane set $(h\ k\ l)$ (3.3)

3.7

$(uvw)^*$

notation for a set of planes in the reciprocal lattice

Note 1 to entry: The normal of the reciprocal plane $(uvw)^*$ is parallel to the crystallographic zone axis $[uvw]$ (3.5).

3.8

reciprocal vector

g_{hkl}

vector in the reciprocal lattice

Note 1 to entry: The reciprocal vector, g_{hkl} , is normal to the crystallographic plane $(h\ k\ l)$ (3.3) with its magnitude inversely proportional to interplanar spacing d_{hkl} (3.6).

3.9

R vector

R_{hkl}

vector from centre, 000 (the origin), to the diffraction spot, hkl , in a diffraction pattern

Note 1 to entry: See [Figure 1](#).

3.10

camera length

L

effective distance between the specimen and the plane where diffraction pattern is formed

[SOURCE: ISO 15932:2010, 3.7]

3.11

camera constant

$L\lambda$

product of the wavelength of the incident electron wave and camera length (3.10)

Note 1 to entry: Because of the small Bragg angle, the Bragg condition can be given in the first-order approximation, $R_{hkl} \cdot d_{hkl} \cong L\lambda$, where d_{hkl} is the interplanar spacing of plane, (hkl) , (3.3) and R_{hkl} (3.9) is the distance of the diffraction spot, hkl , from the incident beam.

[SOURCE: ISO 15932:2010, 3.8, modified]

3.12

bright field image

image formed using only the non-scattered beam, selected by observation of the back focal plane of the objective lens and using the objective aperture to cut out all diffracted beams

[SOURCE: ISO 15932:2010, 5.6]

3.13

dark field image

image formed by a diffracted beam only by using the objective aperture for selection or by collecting the diffracted beam with an annular dark-field detector

[SOURCE: ISO 15932:2010, 5.6]

3.14

energy-dispersive X-ray spectroscopy

EDS

analytical technique which enables the elemental analysis or chemical characterization of a specimen by analysing characteristic X-ray emitted by the matter in response to electron irradiation

[SOURCE: ISO 15932:2010, 6.6]

3.15

eucentric position

specimen position at which the image exhibits minimal lateral motion resulting from specimen tilting

4 Principle

4.1 General

When an energetic electron beam is incident upon a thin crystallographic specimen in a transmission electron microscope, a diffraction pattern will be produced in the back focal plane of the objective lens. This pattern is magnified by the intermediate and projector lenses, then displayed on a viewing screen and recorded (see Reference [3]). This pattern can also be displayed on a monitor if the TEM is equipped with a digital camera system.

4.2 Spot diffraction pattern

The diffraction pattern of a single crystal appears as an array of "spots", the basic unit of which is characterized by a parallelogram. A schematic illustration of a spot diffraction pattern is shown in [Figure 1](#). Each spot corresponds to diffraction from a specific set of crystal lattice planes in the specimen, denoted by Miller indices (hkl) . The vector, R_{hkl} , is defined by the position of the diffracted spot, hkl , relative to position on the pattern corresponding to the transmitted beam, i.e. the centre-spot, 000 , of the pattern. It is parallel to the normal of the reflecting plane, (hkl) . The magnitude of R_{hkl} is inversely proportional to the interplanar spacing, d_{hkl} , of the diffracting plane, (hkl) (see References [4] to [9]). In the context of this document, vectors $R_{h_1k_1l_1}$, $R_{h_2k_2l_2}$, $(R_{h_2k_2l_2} - R_{h_1k_1l_1})$ and $(R_{h_2k_2l_2} + R_{h_1k_1l_1})$ are simplified as R_1 , R_2 , R_{2-1} and R_{1+2} , respectively. The included angle between vectors, R_1 and R_2 , is denoted by γ^* . The basic parallelogram is defined by R_1 and R_2 , where they are the shortest and next shortest in the pattern respectively and not along a common line. The spot, $h_2k_2l_2$, is positioned anticlockwise around the centre spot relative to spot, $h_1k_1l_1$.

Because the centre-spot is often very bright, it is often difficult to determine the exact centre of the pattern. Therefore, a practical procedure is to establish the magnitude of $|R_{hkl}|$ by measuring the distance between the spots, hkl and $\bar{\bar{hkl}}$ on the diffraction pattern and dividing by two, i.e. $|R_{hkl}| = \frac{1}{2}(|R_{hkl}| + |R_{\bar{\bar{hkl}}}|)$. [Figure 2](#) shows an example of the SAED pattern where the magnitude of R_1 , R_2 and R_{2-1} is obtained from $\frac{1}{2}(R_1 + \bar{R}_1)$, $\frac{1}{2}(R_2 + \bar{R}_2)$ and $\frac{1}{2}(R_{2-1} + \bar{R}_{2-1})$ respectively.

The relationship between the interplanar spacing, d_{hkl} , and the magnitude, R_{hkl} , for a reflecting plane, (hkl) , can be approximately expressed as shown in [Formula \(1\)](#) (see References [\[7\]](#) and [\[8\]](#)):

$$L\lambda = R_{hkl} \times d_{hkl} \left[1 - \frac{3}{8} (R_{hkl} / L)^2 \right] = R_{hkl} \times d_{hkl} (1 - \Delta) \quad (1)$$

where

Δ is equal to $\frac{3}{8} (R_{hkl} / L)^2$;

L is the diffraction camera length and equal to $f_o \times M_i \times M_p$;

where

f_o is the focal length, in millimetres, of the objective lens in the microscope;

M_i is the magnification of the intermediate lens;

M_p is the magnification of the projector lenses;

$L\lambda$ is the camera constant (or diffraction constant) of the transmission electron microscope operating under the particular set of conditions. This parameter can be determined from the diffraction pattern of a crystalline specimen of known lattice parameters (see [8.3](#));

λ is the wavelength, in nanometres, of the incident electron beam which is dependent upon the accelerating voltage and can be given by [Formula \(2\)](#) (see Reference [\[4\]](#)):

$$\lambda(\text{nm}) = \frac{1,226}{\sqrt{V(1 + 0,9788 \times 10^{-6} V)}} \quad (2)$$

where V is the accelerating voltage, in volts, of the TEM; the factor in parenthesis is the relativistic correction.

For most work using a TEM, the value of Δ in [Formula \(1\)](#) is usually smaller than 0,1 % and, hence, a more simplified [Formula \(3\)](#) may be used, namely

$$R_{hkl} \cdot d_{hkl} \cong L\lambda \quad (3)$$

For the derivation of the above equation, refer to the textbooks (see References [\[4\]](#) to [\[9\]](#)).

The use of [Formula \(3\)](#) requires measuring the length of R_{hkl} . Since, as mentioned earlier, the location of the pattern centre may not be easily determined; it is recommended that the distance measurement taken, $2R_{h_1k_1l_1}$, be from the $h_1k_1l_1$ diffracted spot to the $\bar{h}_1\bar{k}_1\bar{l}_1$ spot on the pattern. This is equivalent to a diameter measurement on the ring pattern from a polycrystalline specimen. To obtain the interplanar information, the measured distance, $2R_{h_1k_1l_1}$, is halved and [Formula \(3\)](#) applied.

If the camera constant is known, the interplanar spacing, d_{hkl} , of plane, (hkl) , can be calculated. The included angle between any two vectors, $R_{h_1k_1l_1}$ and $R_{h_2k_2l_2}$, can also be measured on the diffraction pattern. This is equal to the angle between the corresponding crystallographic planes, $(h_1k_1l_1)$ and $(h_2k_2l_2)$.

Since diffraction data from a single pattern will provide information on a limited number of the possible diffracting planes in a specimen area, it is necessary to acquire additional diffraction patterns from the same area (or from different grains/particles of the same phase). This requires either the tilting of the specimen or the availability of differently oriented grains or particles of the same phase.

Acquire a second diffraction pattern from another zone axis from the same area by tilting (or tilting and rotating) the specimen so that the two patterns contain a common spot row (see [8.2.10](#) and [Figure 5](#)).

ISO 25498:2018(E)

Index the diffracted spots, and then select three non-planar spots in the two patterns to constitute a reciprocal lattice, which, if the spots correspond to low values of Miller indices, may define the primitive unit cell of the crystal lattice. Therefore, crystal lattice parameters can be determined and the orientation of the grain or particle in the thin specimen can also be calculated.

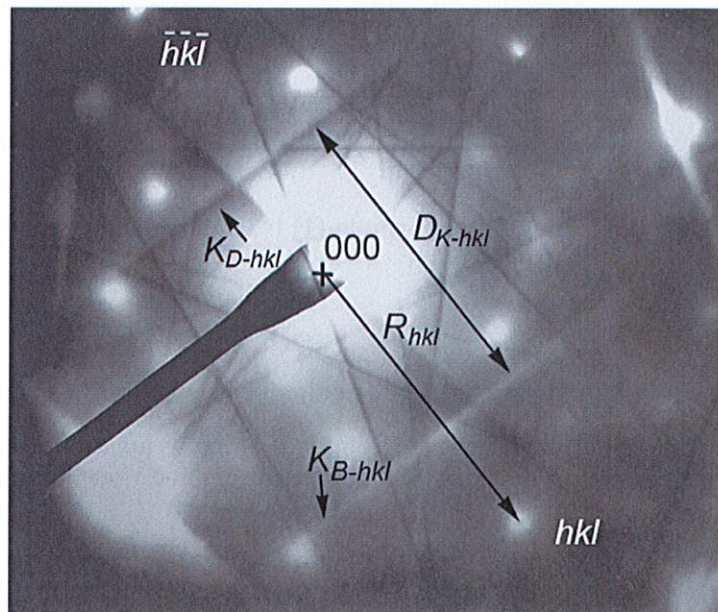
4.3 Kikuchi pattern

When a specimen area is nearly perfect but not thin enough, Kikuchi lines may occur. They arise from electrons scattered inelastically through a small angle and suffering only a very small energy loss being scattered again, this time elastically. This process leads to local variations of the background intensity in the diffraction pattern and the appearance of Kikuchi lines.

The Kikuchi patterns consist of pairs of parallel bright and dark lines, which are parallel to the projection of the corresponding reflecting plane, (hkl) . The bright (excess) line and dark (defect) line in the Kikuchi pattern are denoted by K_{B-hkl} and K_{D-hkl} , respectively. Therefore, the line pair, K_{B-hkl} and K_{D-hkl} , will be perpendicular to the vector, R_{hkl} from the corresponding crystallographic plane (hkl) . Namely they are perpendicular to the reciprocal vector, g_{hkl} , of the plane, (hkl) .

An example of a Kikuchi pattern is given in [Figure 3](#), where the bright line, K_{B-hkl} , and dark line, K_{D-hkl} , pair is superimposed on the spot pattern. The perpendicular distance, D_{K-hkl} , between the line pair, K_{B-hkl} and K_{D-hkl} , is related to the interplanar spacing, d_{hkl} , and camera constant, $L\lambda$, by [Formula \(4\)](#).

$$D_{K-hkl} \cdot d_{hkl} \cong L\lambda \quad (4)$$



Key

- K_{B-hkl} bright line of Kikuchi pair
- K_{D-hkl} dark line of Kikuchi pair
- D_{K-hkl} distance between the line pair K_{B-hkl} and K_{D-hkl}
- +
- centre of the direct beam

Figure 3 — Kikuchi pattern from a steel specimen

The distance between the two Kikuchi lines equals to the distance between the diffraction spot, hkl , and the central spot, 000 . The angles between intersecting Kikuchi pairs are the same as the angles

between their corresponding diffraction spots, and can be measured accurately. These angles are also equal to the angles between the relevant crystallographic planes.

When the specimen is tilted, the diffraction spots only gradually change the brightness, faint or increase the intensity, but their positions are almost at the same place. Instead, Kikuchi lines are sensitive to the tilting. Their movement is significant on the viewing screen. Hence, specimen tilting can be guided by Kikuchi map from one zone axes to another one. The Kikuchi patterns present the real crystal symmetry of the specimen. They can also be used in establishing crystal orientation with a very high accuracy (see References [5] and [9]).

The problem is that Kikuchi patterns cannot always be observed in all of the specimens. In most cases, the SAED studies rely mainly on the spot patterns, though they are not as accurate as Kikuchi patterns.

4.4 Polycrystalline specimen

For randomly oriented aggregates of polycrystals, the diffraction pattern is comprised of a series of concentric rings centred on the spot, 000 , of the direct beam. An example of the pattern from polycrystalline gold (Au) specimen is given in Figure 4. Each diffracted ring arises from the diffraction beams from differently oriented crystallographic planes of the form, $\{hkl\}$; each of these having an identical interplanar spacing. From the diameter of each diffraction ring, the corresponding interplanar spacing, d_{hkl} , can be calculated using Formula (3). Indices of the diffraction rings can be ascribed and then the lattice parameters can also be determined. For the method of indexing ring patterns, refer to that used in X-ray powder diffraction (see Reference [9]).

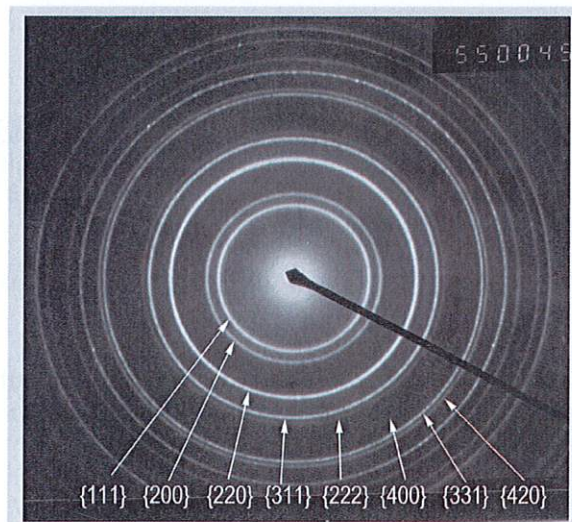


Figure 4 — Diffraction ring pattern with indices from a polycrystalline Au specimen

5 Reference materials

A reference specimen is required for determining the diffraction constant, $L\lambda$, of the microscope in electron diffraction studies. In principle, any thin crystalline foil or powder could be considered as the reference specimen, provided its crystalline structure and lattice parameters have been acquired accurately and they are certified and stable under irradiation of the electron beam. It should be ensured that the reference material, which is as thin as electrons can penetrate through it, has the same crystallographic properties as the bulk material. In addition, a number of sharp diffraction rings or spots with known indices can be observed. The thickness of the crystal foil or powder grain size should be consistent with the beam energy and the quality of the diffraction pattern so that clear diffraction patterns can be observed (when it is too thick, the pattern will lack sharpness).

ISO 25498:2018(E)

Reference materials in common use are polycrystalline specimens made from pure gold [which has a face-centred cubic (FCC) lattice with parameter, $a = 0,407\ 8\ \text{nm}$] or pure aluminium (Al) (FCC structure with lattice parameter $a = 0,404\ 9\ \text{nm}$). The mass fraction of Au or Al in the reference materials shall be not less than 99,9 %. The reference specimen shall be prepared by evaporating a small piece of Au or Al on a grid with a supporting film.

It is also feasible to evaporate a layer of the reference material onto a local surface area of the specimen, which is to be analysed.

6 Equipment

6.1 Transmission electron microscope (TEM) shall be with double tilt or tilt rotation or double-tilt rotate specimen holder.

6.2 Recording of SAED patterns and images.

The SAED patterns and images obtained on the transmission electron microscope shall be recorded on the photographic films or imaging plates or an image sensor built in the digital camera.

When films are used, a darkroom with a negative developing and fixing outfit is required.

6.3 Facilities for specimen preparation.

7 Specimens

7.1 Most specimens are prepared as thin foils (see References [2] and [10]). Such specimens can be obtained in the form of thin sections from a variety of crystalline substances including metallic and non-metallic materials. The shape and external size of the specimen should match that of the TEM specimen holder or, alternatively, it can be held by a support grid.

Fine powders and/or extraction replicas can also be used. These specimens shall be prepared on the grid with supporting films.

7.2 An applicable area to be tested is in the sizes of micrometre and sub-micrometre. The area is always defined by selected aperture. The selected area shall be thin enough for the electron beam to pass through it and diffraction patterns can be observed on the viewing screen.

7.3 The surface of the specimen shall be clean, dry and flat without an oxidizing layer or any contamination.

7.4 For those materials that are stable under energetic particle beam bombardment, contamination on the specimen surface can be avoided or removed by ion beam sputtering or other techniques, such as plasma cleaners, before the TEM observation.

7.5 Prepared specimens shall be labelled and placed in a special specimen box and preserved in a desiccator or evacuated container.

8 Experimental procedure

8.1 Instrument preparation

8.1.1 The general working condition of the TEM laboratory shall comply with ISO/IEC 17025.

ISO 25498:2018(E)

8.1.2 It is recommended to use the cold finger of TEM before conditioning in order to minimize specimen contamination.

8.1.3 When the vacuum of the transmission electron microscope is suitable for operation, switch on and select an appropriate accelerating voltage so that the incident electron beam can penetrate through the specimen.

8.1.4 Carry out the axis alignment for the electron optical system.

8.1.5 The success of the selected area electron diffraction method relies on the validity of indexing the diffraction patterns arising, irrespective of which axis in the specimen lies parallel to the incident electron beam. Such analysis is therefore aided by specimen tilt and rotation facilities.

Place the specimen to be tested and the reference firmly in the double-tilting or tilting-rotation or double-tilting rotation specimen holder, and insert the holder into the specimen chamber.

A specimen coated with an evaporated layer of reference material can be directly placed in the specimen holder and inserted into the chamber.

8.1.6 When the SAED patterns need to be related to features observed in the corresponding micrograph, the angle of rotation between the two may need to be determined and compensated for.

The method in common use is to take a diffraction pattern and a micrograph of a molybdenum trioxide crystal specimen. The rotation angle of the image is then measured on the photographic plates, on which the micrograph and superimposed diffraction pattern has been recorded. For details of the calibration procedure, refer to the appropriate text books (see References [4], [5] and [9]).

When the rotation angle of the TEM has been compensated by the manufacturer, the procedure in [8.1.6](#) may be ignored.

8.1.7 When a digital camera is equipped and to be employed for the study, set the camera in operating condition by following the user's guide of the manufacturer.

To avoid damaging the camera, reduce incident beam intensity and use beam stop to block the central spot when acquiring SAED diffraction patterns.

For detail procedure of the operation and calibration, refer to instruction from the manufacturer.

8.2 Procedure for acquirement of selected area electron diffraction patterns

8.2.1 Obtain a magnified bright field image of the specimen on the viewing screen of the transmission electron microscope. Adjust the specimen height to focus the image so that the image movement is minimized during the tilting of the specimen. Namely, set the eucentric position of the specimen. The procedure for establishing the eucentric position of the specimen may be obtained by consulting the manufacturer's operating manual.

NOTE If the TEM is not equipped with a specimen height control function, this procedure can be omitted.

8.2.2 Adjust the magnification of the specimen image until details in the specimen can be observed clearly. A suitable magnification for SAED analysis is usually from several thousands to tens of thousands times. Focus the image and correct the astigmatism.

8.2.3 Insert the field limiting aperture (selected area aperture) and focus the image of this aperture. Then focus the specimen image again. This makes the selected area aperture plane conjugate with the image plane of the objective lens.

ISO 25498:2018(E)

8.2.4 Switch the microscope from image mode to the SAED mode, focus the image of the objective lens aperture; that is, make this objective lens aperture coincide with the back focal plane of the objective lens. Return to the bright field image mode and focus the image again.

8.2.5 Insert the reference (i.e. the calibration standard) and locate it at the eucentric position. Choose a camera length, L , consistent with the capabilities of the subsequent measuring equipment and then obtain a diffraction pattern from it. Focus the diffraction pattern and correct any astigmatism carefully to make the diffraction pattern sharp. Record the diffraction pattern of the reference.

8.2.6 If the reference and test specimen are not in the same specimen holder, withdraw the reference and insert the test specimen again, without changing the operating conditions and without switching the microscope off. Again, locate it at the eucentric height.

8.2.7 Obtain a focused bright field image of the specimen again with an appropriate magnification.

Select a region of interest (ROI) on the specimen image using the field limiting aperture (selected area aperture). Record the image of this ROI in the specimen. The phase boundaries and/or grain boundaries in the specimen should be kept away from the selected ROI when a single crystal grain is analysed.

8.2.8 Switch the TEM to the SAED diffraction mode again, withdraw the objective lens aperture and obtain a diffraction pattern on the viewing screen. Where possible, tilt the specimen slightly so that the brightness of the spots in the diffraction pattern is evenly distributed, or where Kikuchi lines appear; the Kikuchi line pairs are symmetrical about the pattern centre.

This pattern will then derive from a low index direction in the crystal approximately; the direction is antiparallel to the incident electron beam. This crystal direction will be the zone axis, $[u_1v_1w_1]$, which is the normal of the reciprocal plane, $(u_1v_1w_1)^*$, i.e. the diffraction pattern (see References [4] to [7]).

NOTE The beam direction is defined as antiparallel to the incident electron beam.

Adjust (defocus) the second condenser lens current (the brightness knob) to sharpen the diffraction spots, making them as sharp as possible.

8.2.9 Record the pattern or/and save the original uncompressed pattern in the computer system. Take note of the reading on the X and Y axis of the specimen tilting device as X_1 and Y_1 , respectively. Using dark field conditions either by beam tilt or shifting the objective lens aperture, identify the source of the pattern.

8.2.10 Insert the reference specimen and obtain a second diffraction pattern from the reference. Record this diffraction pattern (see also 8.3), making sure that the same experimental conditions are used (i.e. accelerating voltage, lens settings and, especially, the specimen height and camera length, L).

8.2.11 Obtain sufficient data for each phase of interest by either of the following procedures.

a) Specimen tilting procedure: obtain the second pattern by tilting the specimen.

Choose a row of close-spaced diffraction spots collinear with the central transmitted spot on the diffraction pattern, which is denoted by indices of reciprocal plane, $(u_1v_1w_1)^*$. Keep this row of the spots visible on the viewing screen, while tilting the specimen until the second diffraction pattern, $(u_2v_2w_2)^*$ appears. Make sure the brightness of the spots in the second pattern is evenly distributed. The reciprocal space geometry of the two patterns is schematically illustrated in [Figure 5](#). The angle between the diffraction patterns, $(u_1v_1w_1)^*$ and $(u_2v_2w_2)^*$, is Ψ , which equals to the angle between the two zone axes, $[u_1v_1w_1]$ and $[u_2v_2w_2]$. This angle can be determined from the tilt angle of the specimen holder.

ISO 25498:2018(E)

If Kikuchi patterns are visible, the specimen tilting can be guided by the Kikuchi map. The second diffraction pattern (or more patterns) may be obtained directly.

With a rotate-tilt specimen holder or a double-tilting rotate holder, a chosen row of the spots can be aligned with a tilt axis; the second diffraction pattern (or more patterns) may be obtained directly.

Repeat the procedure described in [8.2.8](#), recording the pattern and/or saving it on the computer system. Take note of the reading on the X and Y axis of the specimen-tilting device as X_2 and Y_2 , respectively.

- b) Multi grains procedure: obtain the patterns from several areas, i.e. different particles or grains of the same phase. This procedure is recommended for any of the following situations:
- 1) the maximum tilting angle of the specimen holder is not large enough, so that the second diffraction pattern cannot be reached by tilting;
 - 2) the particles to be analysed in the specimen are too small;
 - 3) the specimen is sensitive to the electron beam illumination, e.g. the selective area is contaminated or decomposes following a short irradiation by the electron beam.

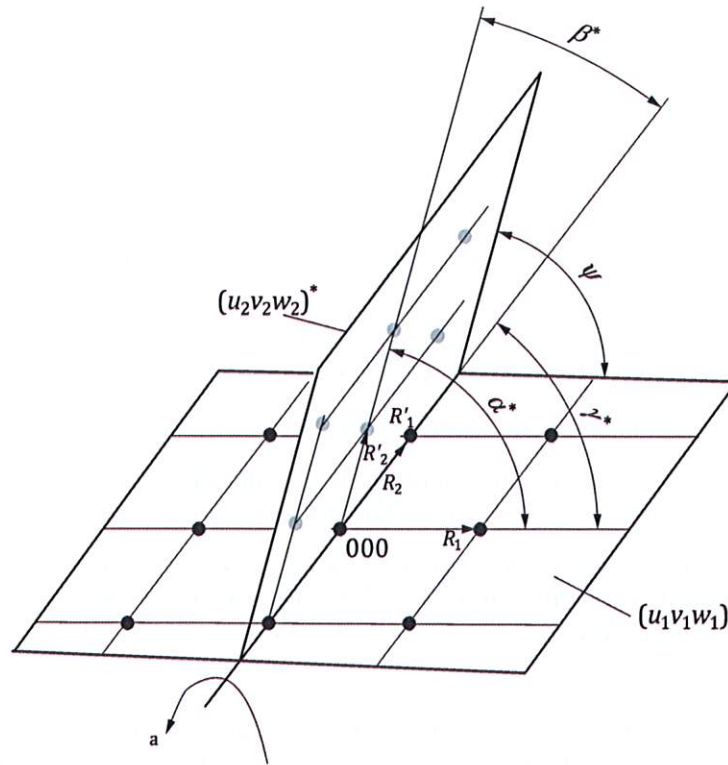
When this procedure is employed, the source of each diffraction pattern is necessary to confirm. Choose appropriate diffraction spots to form a dark field image to check it. Further confirmation can be achieved through simultaneous use of an EDX (energy dispersive X-ray spectrometry) facility, when available.

8.2.12 When the diffraction patterns are recorded on negative films, develop, fix and dry the films in the darkroom. Keep the negative films one by one in individual protective bags with labels.

8.2.13 When the diffraction patterns are recorded by digital camera or imaging plates, save the original uncompressed diffraction patterns in the computer system as individual files with labels. All parameters of the acquisition of this file shall be documented and reported.

8.2.14 Each pattern, either recorded on negative film or by digital camera as well as by imaging plate, shall be numbered and labelled with the following information: specimen designation and serial number, accelerating voltage, nominal camera length, L , tilting angles, operator, date, etc. All processing operations of the diffraction patterns and images shall be reported.

ISO 25498:2018(E)



Key

ψ angle between the diffraction pattern $(u_1v_1w_1)^*$ and $(u_2v_2w_2)^*$

$R_1' = R_2$

a Tilting axis.

Figure 5 — Reciprocal space geometry of the spot diffraction patterns

8.3 Determination of diffraction constant, $L\lambda$

8.3.1 The procedure for the determination of the diffraction constant uses a reference specimen such as polycrystalline pure gold or pure aluminium (see Clause 7). Figure 4 shows an example of the ring patterns from a polycrystalline gold specimen. Record the diffraction pattern (see 8.2).

8.3.2 When diffraction patterns are recorded on photographic films, place the negative film on which the diffraction pattern of the reference specimen was recorded, emulsion side up on the film viewer. Measure the diameters of the diffraction rings on the film of the reference specimen when a polycrystalline reference is used. Note the diameter of these rings from inner to outer as $D_1, D_2, D_3, D_4, \dots$ (mm), etc., respectively.

8.3.3 Indices, hkl , of the diffraction rings for a reference specimen with FCC structure are 111, 200, 220, 311, 222, 400, 331, 420, 422, ... respectively from the inner to outer rings (see Figure 4). The corresponding interplanar spacings, d_{hkl} , are given for both Au and Al in Annex A or calculated by the crystallographic formulae (see References [4] to [9]).

8.3.4 According to [Formula \(3\)](#), calculate the diffraction constants as follows:

$$L_1 \lambda = D_1 \cdot d_{111} / 2 \quad (\text{mm} \cdot \text{nm})$$

$$L_2 \lambda = D_2 \cdot d_{200} / 2 \quad (\text{mm} \cdot \text{nm})$$

$$L_3 \lambda = D_3 \cdot d_{220} / 2 \quad (\text{mm} \cdot \text{nm}) \dots, \text{etc.}$$

8.3.5 Plot the $L\lambda - D/2$ curve using the data in [8.3.2](#) and [8.3.4](#) (an example of the $L\lambda - D/2$ plot is shown in [Figure 6](#)). This graph could be used for all reflections (spots) from the specimen being analysed under completely identical conditions. Since the diffraction constant, $L\lambda$, actually varies slightly with the diffraction ring diameter, it is recommended either

- to use the $L\lambda - D/2$ curve to obtain the value of $L\lambda$ corresponding to the same distance, $D/2$, as the spot being measured, or
- to use an average value of the camera constant and subsequently make allowance for the small uncertainty this will produce in the d -value obtained.

8.3.6 When the diffraction patterns are recorded by the digital camera, the above measurements and calculations can be carried out by the computer system.

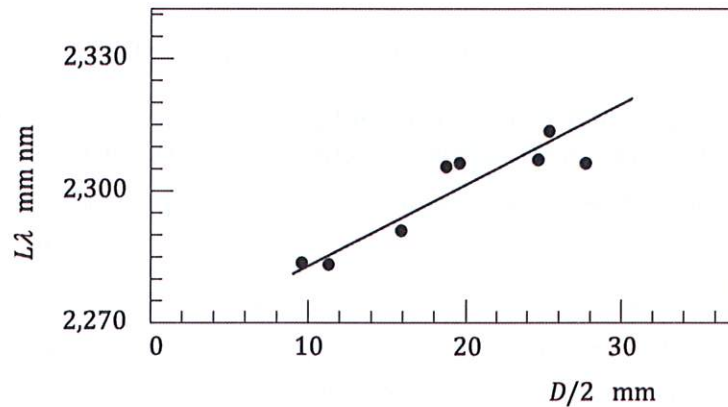


Figure 6 — $L\lambda - D/2$ curve from a polycrystalline Au specimen

9 Measurement and solution of the SAED patterns

9.1 Selection of the basic parallelogram

9.1.1 When photographic films are used for recording diffraction patterns, place the film, on which the diffraction pattern was recorded, on the film viewer with its emulsion side up.

9.1.2 Select two diffracted spots, $h_1 k_1 l_1$ and $h_2 k_2 l_2$, from the diffraction pattern with zone axis, $[u_1 v_1 w_1]$, such that these spots are the nearest and next nearest to the central spot, 000 , respectively. They shall not be collinear with the centre-spot, 000 . The spot, $h_2 k_2 l_2$, is positioned anticlockwise

ISO 25498:2018(E)

around the centre spot relative to spot, $h_1k_1l_1$. The two diffracted spots, the centre-spot and the spot, $(h_1 + h_2, k_1 + k_2, l_1 + l_2)$, constitute a parallelogram (see [Figure 1](#)).

Measure the distance, $2R_1$ between the spots, $h_1k_1l_1$ and $\bar{h}_1\bar{k}_1\bar{l}_1$, and the distance, $2R_2$, between the spots, $h_2k_2l_2$ and $\bar{h}_2\bar{k}_2\bar{l}_2$, to get the magnitude of the vectors, R_1 and R_2 (see [Figures 1](#) and [2](#)). The corresponding angle, γ^* , between R_1 and R_2 shall also be measured.

Where individual patterns are obtained, obtain the magnitude of the vectors, R_{1+2} and R_{2-1} (see [Figures 1](#) and [2](#)). The angles between \bar{R}_1 and R_{2-1} , between R_{2-1} and R_2 and the angle between \bar{R}_1 and R_2 shall be measured. These are ϕ_3 , ϕ_2 and ϕ_1 respectively, and $\phi_3 + \phi_2 = \phi_1$.

9.1.3 The angles ϕ_3 , ϕ_2 and ϕ_1 can be calculated using [Formulae \(5\)](#), [\(6\)](#) and [\(7\)](#):

$$\phi_1 = \cos^{-1} \left[\left(R_1^2 + R_2^2 - R_{1+2}^2 \right) / 2R_1R_2 \right] \quad (5)$$

$$\phi_2 = \cos^{-1} \left[\left(R_2^2 + R_{2-1}^2 - R_1^2 \right) / 2R_2R_{2-1} \right] \quad (6)$$

$$\phi_3 = \cos^{-1} \left[\left(4R_1^2 + R_{2-1}^2 - R_{1+2}^2 \right) / 4R_1R_{2-1} \right] \quad (7)$$

If $\phi_1 = \phi_2 + \phi_3$ within the tolerances set by the uncertainty, then proceed; otherwise, check R_s and ϕ_s .

9.1.4 Perform the same procedure as described in [9.1.3](#) on the second diffraction pattern with zone axis, $[u_2v_2w_2]$ (and on any others from different directions of the specimen). The basic parallelogram on the second pattern is constituted by R'_1 and R'_2 and the centre-spot, 000 . The vector, R'_1 , shall be superimposed over the vector, R_2 , of the pattern with zone axis, $[u_1v_1w_1]$, i.e. $R'_1 = R_2$ (see [Figure 5](#)). Measure the magnitude of R'_1 and R'_2 as well as the angle, β^* , between R'_1 and R'_2 . The vectors, R_1 , R_2 and R'_2 constitute a basic cell of the reciprocal space. If the corresponding diffraction spots possess the lowest indices, then the reciprocal unit cell can be obtained.

9.1.5 When a digital camera is employed, measurement and calculation on the diffraction patterns can be carried out by the computer system.

9.1.6 The angle, α^* , between R_1 and R'_2 (see [Figure 5](#)) may be calculated using [Formula \(8\)](#):

$$\cos \alpha^* = \sin \gamma^* \times \sin \beta^* \times \cos \psi + \cos \gamma^* \times \cos \beta^* \quad (8)$$

where

β^* is the angle between R'_1 and R'_2 ;

γ^* is the angle between R_1 and R_2 ;

ψ is the angle between the diffraction patterns, $(u_1v_1w_1)^*$ and $(u_2v_2w_2)^*$, or the zone axes, $[u_1v_1w_1]$ and $[u_2v_2w_2]$.

9.2 Indexing diffraction spots

9.2.1 Use [Formula \(3\)](#) to calculate the interplanar spacing, d_{hkl} , corresponding to the above diffraction spots. The interplanar spacing, d_{hkl} , can also be acquired by measuring the distance, D_{K-hkl} , between the Kikuchi bright and dark line pair and using [Formula \(4\)](#).

9.2.2 Arbitrarily index two of the spots, say $(h_1k_1l_1)$ and $(h_2k_2l_2)$, and then confirm from the possible indices of the other spots that:

$$h_3 = h_2 - h_1, k_3 = k_2 - k_1, l_3 = l_2 - l_1, \text{ and}$$

$$h_4 = h_2 + h_1, k_4 = k_2 + k_1, l_4 = l_2 + l_1.$$

Make any allowance for the multiplicity of $\{h_jk_jl_j\}$. If no solution is possible, then recheck the determination of d_i and the angles (see [9.1.3](#)) until one is found that satisfies these requirements within the tolerances. All spots in a continuous pattern will come from a common zone, $[uvw]$, and have a common axis. This direction is given by [Formula \(9\)](#). The direction, $[uvw]$, can be checked since for all (hkl) 's indexed

$$hu + kv + lw = 0 \tag{9}$$

9.2.3 Calculate the characteristic parameters of the two-dimensional primitive cell on each reciprocal lattice plane of the crystal specimen in advance, namely the indices, $h_1k_1l_1$ and $h_2k_2l_2$, of the primitive reciprocal vector, g_1 and g_2 , ratio of the magnitudes, $g_2:g_1$, the included angle between the vectors g_1 and g_2 and the zone axis index.

The zone axis index, $[uvw]$, can be obtained using [Formula \(10\)](#):

$$u:v:w = \left(\begin{array}{c|c|c} k_1 & l_1 & l_1 \\ \hline k_2 & l_2 & l_2 \end{array} \middle| \begin{array}{c|c|c} h_1 & k_1 & k_1 \\ \hline h_2 & k_2 & k_2 \end{array} \right) = [(k_1l_2 - l_1k_2):(l_1h_2 - h_1l_2):(h_1k_2 - k_1h_2)] \tag{10}$$

The values of u , v , w should be integers without a common factor. The zone axis index, $[uvw]$, is in terms of the normal of reciprocal plane. It shall be converted to the crystallographic direction index, $[UVW]$, in real space by the crystallographic relation. The crystallographic formulae usually can be obtained from the literature and/or handbooks (such as References [\[4\]](#), [\[5\]](#), [\[6\]](#), [\[7\]](#) and [\[9\]](#)). Only for cubic crystals the index, $[uvw]$, of the reciprocal space are not needed to convert, which is equal to the index, $[UVW]$, in the real space.

For the convenience of users of this document, the standard spot patterns of cubic systems and a close-packed hexagonal system with low indices are given in [Annex B](#). For those specimens with a lower symmetry, reference to a diffraction database such as "The Powder Diffraction File 1997–2007", published by the International Centre for Diffraction Data (ICDD), is recommended (see Reference [\[11\]](#)). Software is also very useful in establishing the reciprocal planes of the crystal specimen, especially in one with low symmetry structure (see References [\[4\]](#) and [\[9\]](#)).

For an unknown specimen, the chemical composition should also be determined by microanalysis (e.g. EDX analysis) and/or chemical analysis so that the specimen phase can be identified.

9.2.4 Compare the geometrical characteristics of the experimental diffraction patterns, including the ratio, R_2/R_1 and R_{2-1}/R_1 , the included angle between R_1 , R_2 and R_{2-1} , respectively, with the calculated characteristic parameters of the primitive cell. If the experimental value is consistent with the known value within error, the diffraction spots can be indexed as $h_1k_1l_1$, $h_2k_2l_2$ and

ISO 25498:2018(E)

$(h_2 - h_1, k_2 - k_1, l_2 - l_1)$, respectively. The indices of other diffraction spots can be obtained by the summation of the corresponding vectors. Therefore, the zone axis index, $[uvw]$, can be worked out.

9.2.5 For beam-sensitive nanocrystals, it is often incapable to collect a tilting series of the diffraction patterns from a single nanocrystal. The method that uses randomly oriented diffraction patterns with unknown angular relationships may apply. The key point of this approach is to construct a principal facet by the lengths of the two basis vectors and the angle between them in the diffraction pattern. Based on matching the observed crystal facets to model facets extracted from a simulated three-dimensional lattice, the potential unit cell can be determined. The diffraction pattern can also be indexed. For detail procedure of this algorithm, refer to references (see References [12] and [13]).

10 180° ambiguity

The indices in a diffraction pattern with only one zone axis from a single crystal are not decided uniquely because of the 180° ambiguity created by the diffraction effect. Therefore, the spots, $h_1k_1l_1$ and $h_2k_2l_2$, can also be indexed as $\bar{h}_1\bar{k}_1\bar{l}_1$ and $\bar{h}_2\bar{k}_2\bar{l}_2$, respectively, and vice versa, except that higher Laue zone diffraction spots can be obtained.

However, this ambiguity may be removed by the following methods.

- a) After recording a diffraction pattern, $[u_1v_1w_1]$, tilt the specimen while keeping a row of spots bright, containing the central spot, until another zone axis pattern, $[u_2v_2w_2]$, appears. Record the second pattern and determine the included angle between the two patterns (see 8.2.11). Index the two patterns so that all the indices are entirely self-consistent. The angle between the two patterns shall coincide with the tilting angle.
- b) Obtain a diffraction pattern with zone axis, $[u_1v_1w_1]$, which is superposed on another pattern, $[u_2v_2w_2]$, from the same crystal. Index the two patterns self consistently.
- c) Tilt the specimen to get three non-parallel Kikuchi line pairs in one pattern. Unambiguous indices can be gained.

11 Uncertainty estimation

11.1 Factors affecting accuracy

The camera constant will change if the high voltage supply to the electron microscope fluctuates. Normally, stabilization ratios are 10^5 to 1 or better and thus, this effect is minimal.

As discussed in [Clause 4](#), the effective camera length is defined as [Formula \(11\)](#) (see Reference [7]):

$$L = f_o \times M_i \times M_p \quad (11)$$

where

M_i is the magnification of the intermediate lens;

M_p is the magnification of the projector lens;

f_o is the focal length of the objective lens, the most sensitive factor which affects the reproducibility of L .

In turn, f_o depends on the plane of the object. The factors that control this are specimen holders of different length, support grids that are not flat, thick and buckled specimens, and the effects due to tilting the specimen.

Faulty lens settings will alter $2L\lambda$ if the correct procedure for obtaining diffraction settings is not followed. It can be shown in [Formula \(12\)](#):

$$\frac{\Delta L}{L} = \frac{\Delta f_o}{f_o} + \frac{\Delta M_i}{M_i} + \frac{\Delta M_p}{M_p} \quad (12)$$

where

$\Delta L/L$ is the proportional error in the camera length, L ;

$\Delta f_o/f_o$ is the proportional error in the focal length f_o of the objective lens;

$\Delta M_i/M_i$ is the proportional error in the magnification of the intermediate lens;

$\Delta M_p/M_p$ is the proportional error in the magnification of the projector lens.

In some instruments, the strength of the projector lens is fixed so that $\Delta M_p / M_p = 0$. However, in other instruments, the projector current is variable and the accuracy of the setting has a marked effect on $2L\lambda$. $\Delta M_i/M_i$ is the error in re-adjusting the intermediate lens strength to image the diffraction pattern from the back focal plane of the objective lens. This adjustment can be made with considerable accuracy, so $\Delta M_i/M_i$ is usually very small.

11.2 Calibration with a reference material

Measurement of “ d ” spacing involves the use of a reference material so that the camera constant, $2L\lambda$, can be determined and the effects of variation in microscope parameters can be ignored, provided the conditions for obtaining the diffraction pattern of the standard and unknown are identical. Thus, the main errors involved in the determination of the camera constant, and consequently the d values, arise from inaccuracies in the measurement of rings and spots.

Lens aberration may lead to distortion of diffraction rings into ellipses and thus, measurements of diameter shall be made at least six positions when determining the $L\lambda - D/2$ curve to determine the minimum and maximum values of the diameters (see [8.3.5](#)). Thus, the standard deviation in the camera constant value, S_{cc} , can be determined from this calibration curve. Errors involved in the determination of the spot or ring diameters can be estimated from replicate measurements of these values and an evaluated standard deviation, S_d . This uncertainty shall be combined with the calibration uncertainty associated with the measuring instrument, S_m , and thus yield an uncertainty related to spot or ring dimensions. Thus, the combined uncertainty for determination of d values is expressed by [Formula \(13\)](#).

$$u = \sqrt{(s_{cc})^2 + (s_d)^2 + (s_m)^2} \quad (13)$$

ISO 25498:2018(E)

Annex A
 (informative)

Interplanar spacing

A.1 Interplanar spacing of pure Au and Al

The interplanar spacings, d_{hkl} , of pure gold and aluminium are listed in [Table A.1](#).

Table A.1 — Interplanar spacing, d_{hkl} , of pure Au and Al

Dimensions in nanometres

Miller indices of crystallographic planes	Interplanar spacing of Au d_{hkl}	Interplanar spacing of Al d_{hkl}
{111}	0,235 50	0,233 80
{200}	0,203 90	0,202 40
{220}	0,144 20	0,143 10
{311}	0,123 00	0,122 10
{222}	0,117 74	0,116 90
{400}	0,101 96	0,101 24
{331}	0,093 58	0,092 89
{420}	0,091 20	0,090 55
{422}	0,083 25	0,082 66
{333}/{511}	0,078 00	—

NOTE 1 Lattice parameter for Au [face-centred cubic (FCC) structure, S.G: Fm3m(225)]: $a = 0,407\ 8\ \text{nm}$. See Reference [\[14\]](#).

NOTE 2 Lattice parameter for Al [FCC structure, S.G: Fm3m(225)]: $a = 0,404\ 9\ \text{nm}$. See Reference [\[14\]](#).

Annex B (informative)

Spot diffraction patterns of single crystals for BCC, FCC and HCP structure [7]

B.1 Symbols and definitions

B.1.1 Zone axis, $[uvw]$

In a spot diffraction pattern, the symbol $[uvw]$ denotes index of the zone axis, which is the normal of this diffraction pattern.

B.1.2 Regulation for the reciprocal vectors

In this document, the symbols R_1 and R_2 of the R vectors in a spot diffraction pattern are specified as follows:

R_1 is the shortest vector in the diffraction pattern;

R_2 is the next shortest vector, which is not along a common line with R_1 and is positioned anticlockwise around the centre spot relative to R_1 . The relation between the vectors is as follows:

$$R_3 = R_2 - R_1 \text{ and } R_3 \geq R_2 \geq R_1.$$

B.2 Spot diffraction patterns for body-centred cubic (BCC) crystal, $(u^2+v^2+w^2 \leq 22)$

Spot diffraction patterns from a single crystal with BCC structure are given in [Figures B.1](#) to [B.15](#).

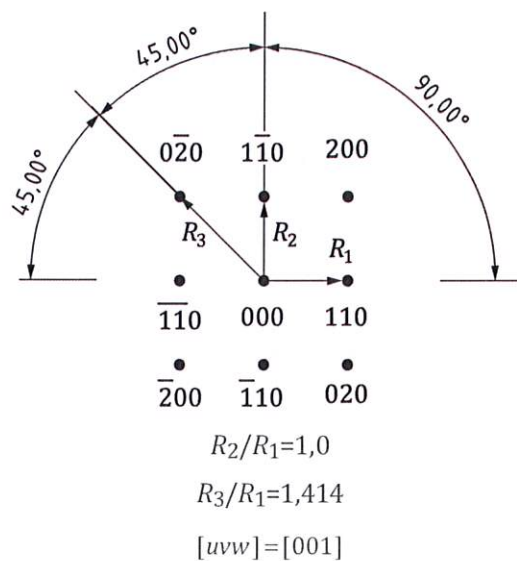


Figure B.1

ISO 25498:2018(E)

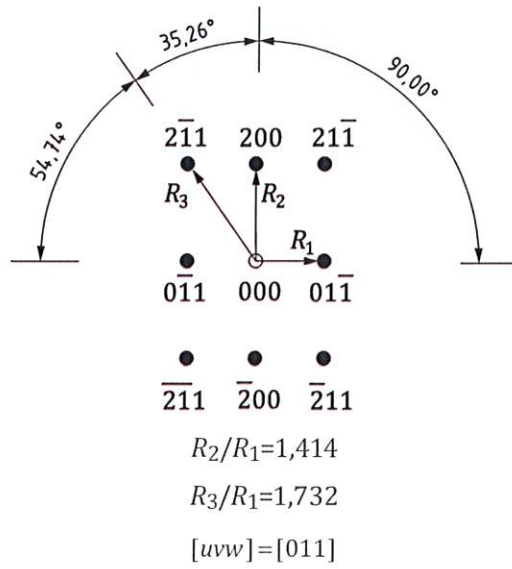


Figure B.2

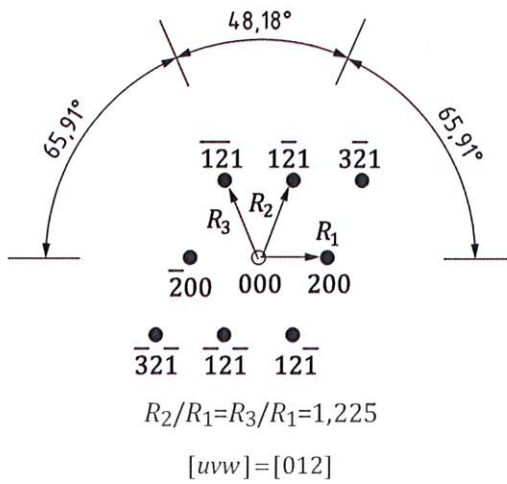
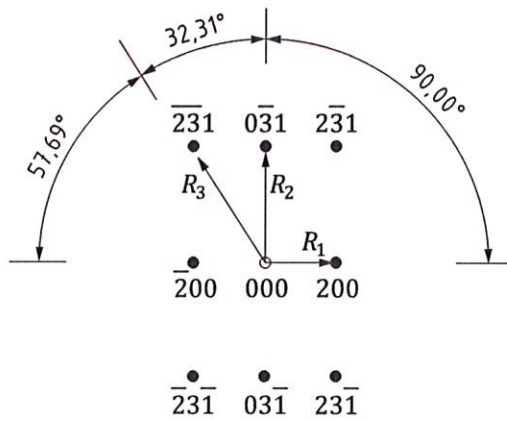


Figure B.3

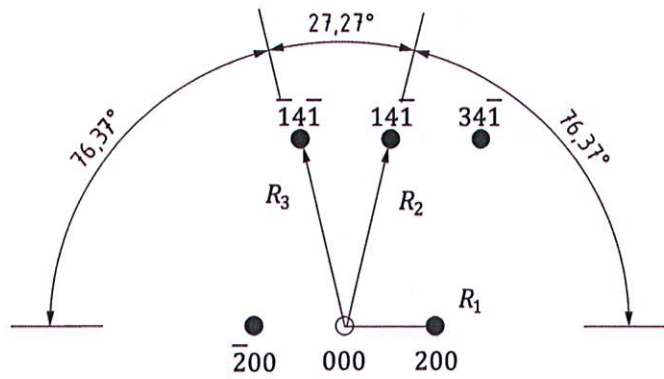


$$R_2/R_1=1,581$$

$$R_3/R_1=1,871$$

$$[uvw]=[013]$$

Figure B.4



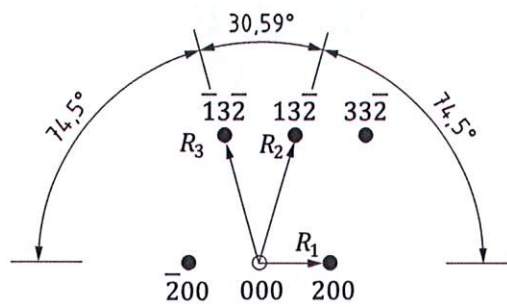
$$\begin{array}{ccc} \bullet & \bullet & \bullet \\ \hline 341 & 141 & 141 \end{array}$$

$$R_2/R_1=2,121$$

$$R_3/R_1=2,121$$

$$[uvw]=[014]$$

Figure B.5



$$\begin{array}{ccc} \bullet & \bullet & \bullet \\ \hline 332 & 132 & 132 \end{array}$$

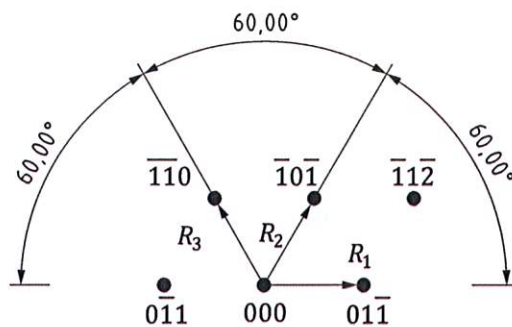
$$R_2/R_1=1,871$$

$$R_3/R_1=1,871$$

$$[uvw]=[023]$$

Figure B.6

ISO 25498:2018(E)



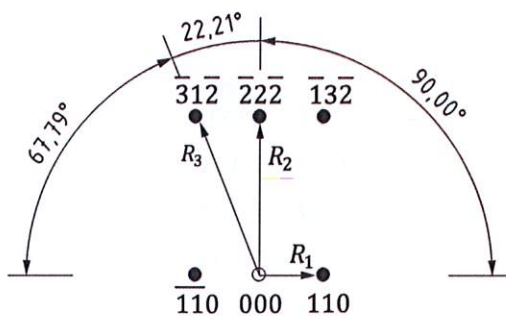
$\bar{1}\bar{1}\bar{2}$ $\bar{1}\bar{0}\bar{1}$ $\bar{1}\bar{1}\bar{0}$

$R_2/R_1=1,0$

$R_3/R_1=1,0$

$[uvw]=[\bar{1}\bar{1}\bar{1}]$

Figure B.7



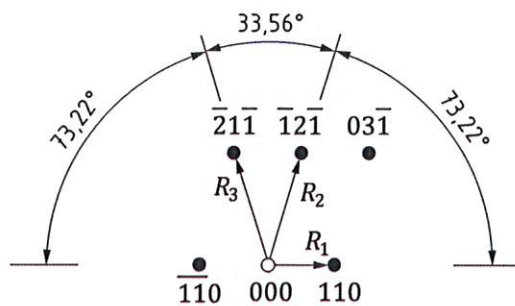
$\bar{1}\bar{3}\bar{2}$ $\bar{2}\bar{2}\bar{2}$ $\bar{3}\bar{1}\bar{2}$

$R_2/R_1=2,450$

$R_3/R_1=2,646$

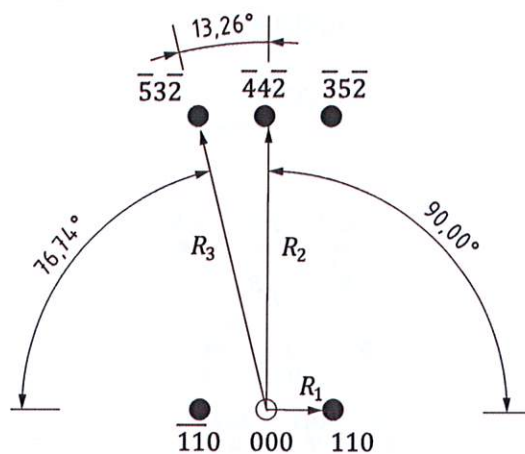
$[uvw]=[\bar{1}\bar{1}\bar{2}]$

Figure B.8



\bullet \bullet \bullet
 $0\bar{3}1$ $1\bar{2}1$ $2\bar{1}1$
 $R_2/R_1=1,732$
 $R_3/R_1=1,732$
 $[uvw]=[\bar{1}13]$

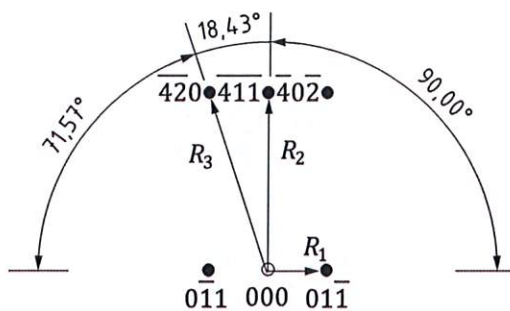
Figure B.9



\bullet \bullet \bullet
 $3\bar{5}2$ $4\bar{4}2$ $5\bar{3}2$
 $R_2/R_1=4,243$
 $R_3/R_1=4,359$
 $[uvw]=[\bar{1}14]$

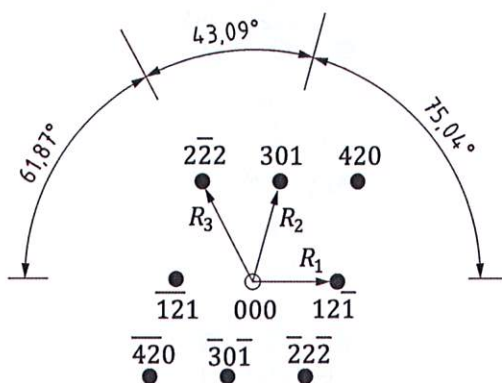
Figure B.10

ISO 25498:2018(E)



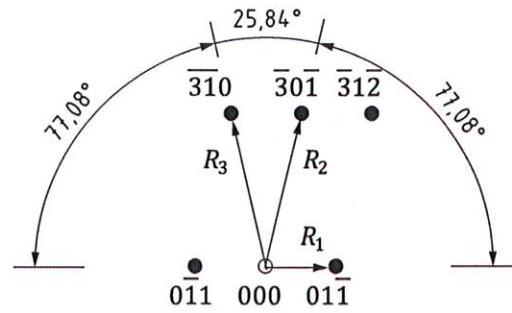
\bullet \bullet \bullet
 402 411 420
 $R_2/R_1=3,0$
 $R_3/R_1=3,162$
 $[uvw]=[\bar{1}22]$

Figure B.11



$R_2/R_1=1,291$
 $R_3/R_1=1,826$
 $[uvw]=[\bar{1}23]$

Figure B.12



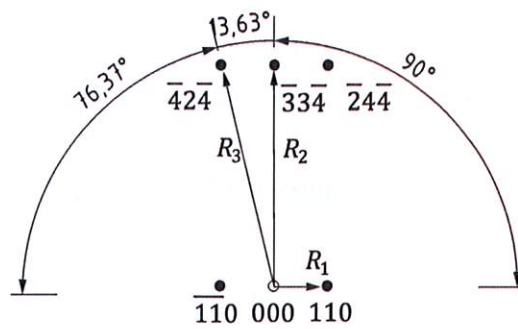
$\bar{3}12$ 301 310
 ● ● ●

$$R_2/R_1=2,236$$

$$R_3/R_1=2,236$$

$$[uvw]=[\bar{1}33]$$

Figure B.13



$\bar{2}44$ $\bar{3}34$ $\bar{4}24$
 ● ● ●

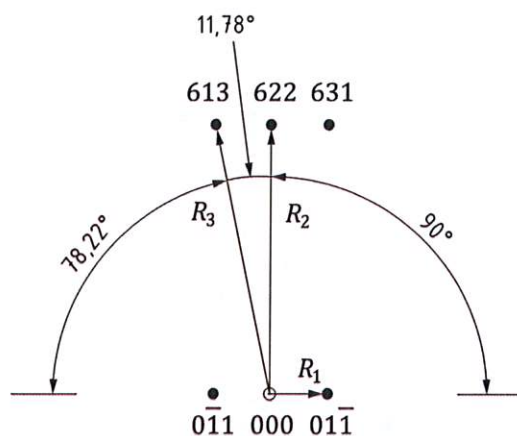
$$R_2/R_1=4,123$$

$$R_3/R_1=4,243$$

$$[uvw]=[\bar{2}23]$$

Figure B.14

ISO 25498:2018(E)

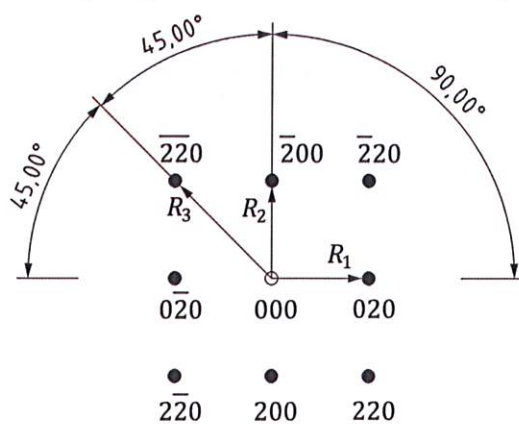


$\overline{631}$ $\overline{622}$ $\overline{613}$
 $R_2/R_1=4,690$
 $R_3/R_1=4,796$
 $[uvw]=[\overline{233}]$

Figure B.15

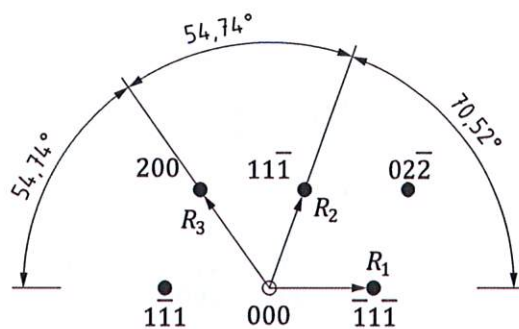
B.3 Spot diffraction patterns for face-centred cubic (FCC) structure
 $(u^2+v^2+w^2 \leq 22)$

Spot diffraction patterns from a single crystal with FCC structure are given in [Figures B.16 to B.30](#).



$R_2/R_1=1,00$
 $R_3/R_1=1,414$
 $[uvw]=[001]$

Figure B.16



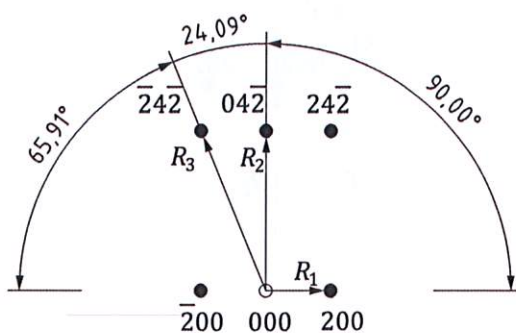
\bullet \bullet \bullet
 $\bar{0}22$ $\bar{1}11$ $\bar{2}00$

$R_2/R_1=1,000$

$R_3/R_1=1,155$

$[uvw]=[011]$

Figure B.17



\bullet \bullet \bullet
 $\bar{2}42$ $\bar{0}42$ $\bar{2}42$

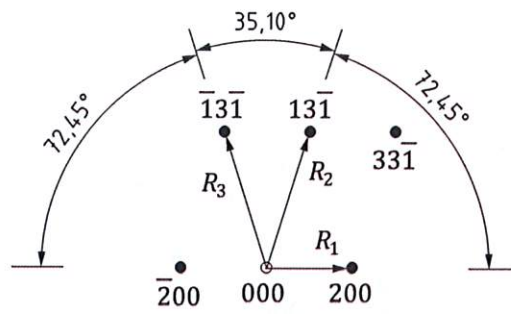
$R_2/R_1=2,236$

$R_3/R_1=2,450$

$[uvw]=[012]$

Figure B.18

ISO 25498:2018(E)



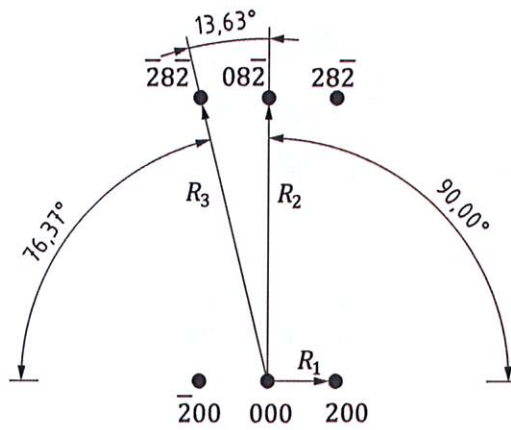
$\bar{3}31$ $\bar{1}31$ $\bar{1}31$

$R_2/R_1=1,658$

$R_3/R_1=1,658$

$[uvw]=[013]$

Figure B.19



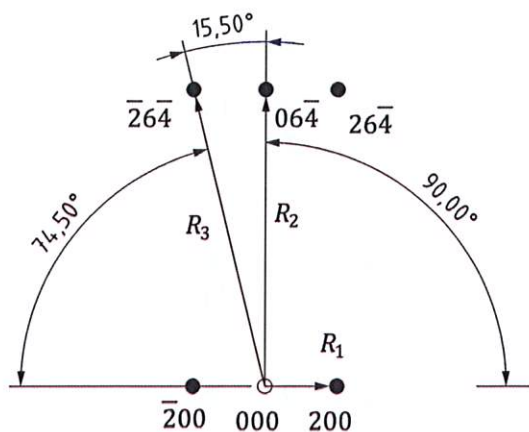
$\bar{2}82$ $\bar{0}82$ $\bar{2}82$

$R_2/R_1=4,123$

$R_3/R_1=4,243$

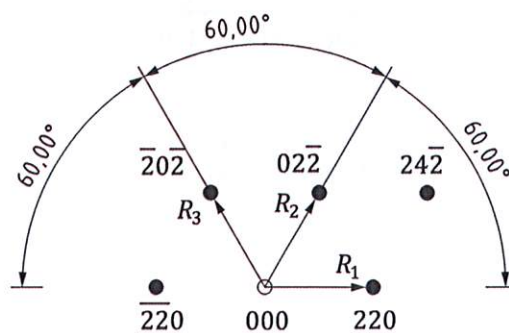
$[uvw]=[014]$

Figure B.20



$\overline{264}$ $\overline{064}$ $\overline{264}$
 ● ● ●
 $R_2/R_1=3,242$
 $R_3/R_1=3,606$
 $[uvw]=[023]$

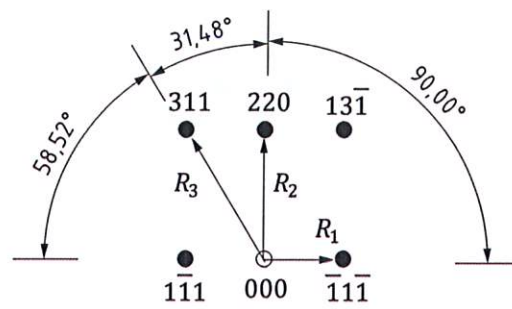
Figure B.21



● ● ●
 $\overline{242}$ $\overline{022}$ $\overline{202}$
 $R_2/R_1=1,00$
 $R_3/R_1=1,00$
 $[uvw]=[111]$

Figure B.22

ISO 25498:2018(E)

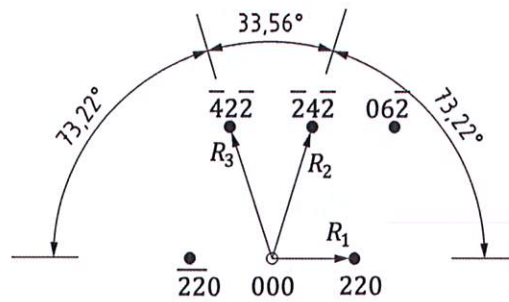


$R_2/R_1=1,633$

$R_3/R_1=1,915$

$[uvw]=[\bar{1}12]$

Figure B.23

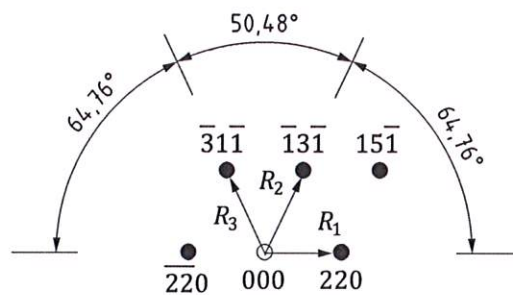


$R_2/R_1=1,732$

$R_3/R_1=1,732$

$[uvw]=[\bar{1}13]$

Figure B.24

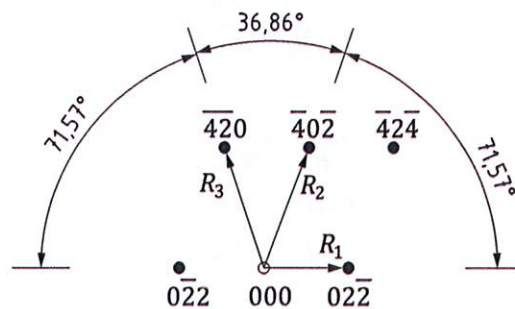


$$R_2/R_1=1,173$$

$$R_3/R_1=1,173$$

$$[uvw]=[\bar{1}14]$$

Figure B.25



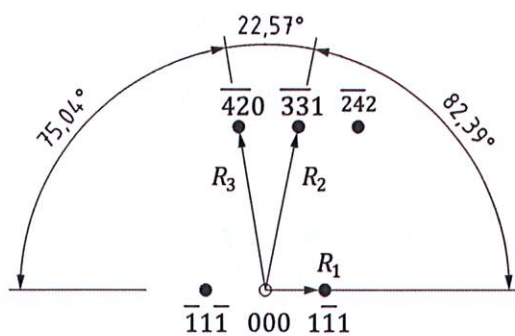
$$\begin{array}{ccc} \bullet & \bullet & \bullet \\ \bar{4}24 & 402 & 420 \\ \bullet & \bullet & \bullet \end{array}$$

$$R_2/R_1=1,581$$

$$R_3/R_1=1,581$$

$$[uvw]=[\bar{1}22]$$

Figure B.26



$$\begin{array}{ccc} \bullet & \bullet & \bullet \\ 242 & 331 & 420 \\ \bullet & \bullet & \bullet \end{array}$$

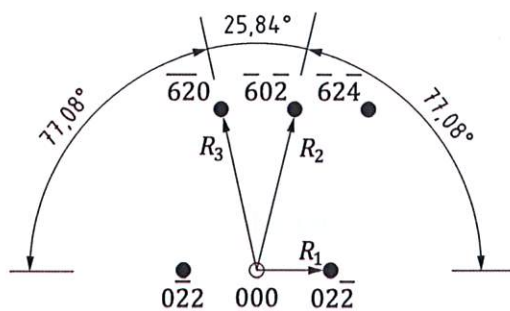
$$R_2/R_1=2,517$$

$$R_3/R_1=2,828$$

$$[uvw]=[\bar{1}23]$$

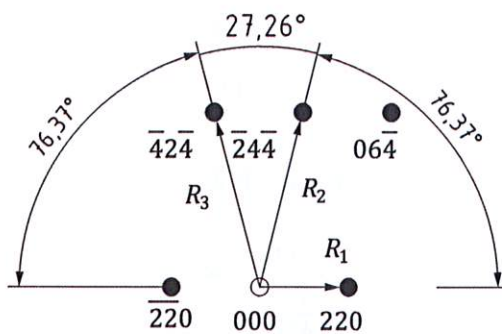
Figure B.27

ISO 25498:2018(E)



$\bar{6}24$ 602 620
 $R_2/R_1=2,236$
 $R_3/R_1=2,236$
 $[uvw]=[133]$

Figure B.28



$\bar{0}64$ $\bar{2}44$ $\bar{4}24$
 $R_2/R_1=2,121$
 $R_3/R_1=2,121$
 $[uvw]=[\bar{2}23]$

Figure B.29

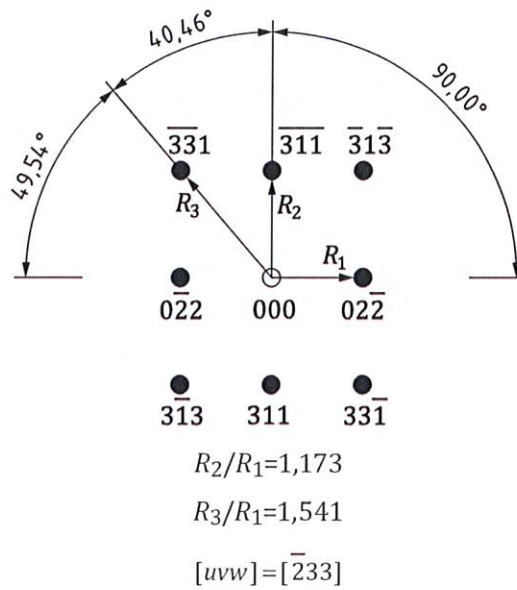


Figure B.30

B.4 Spot diffraction patterns for hexagonal close-packed (HCP) structure for $c/a \cong 1,633$

Spot diffraction patterns from single crystal with HCP structure (for $c/a = \sqrt{8/3} \cong 1,633$) are given in [Figures B.31](#) to [B.40](#). Miller-Bravais index is used for indexing the diffraction patterns of HCP crystals.

NOTE The symbol, ×, denotes the forbidden diffracted spots, which can occur due to the secondary diffraction.

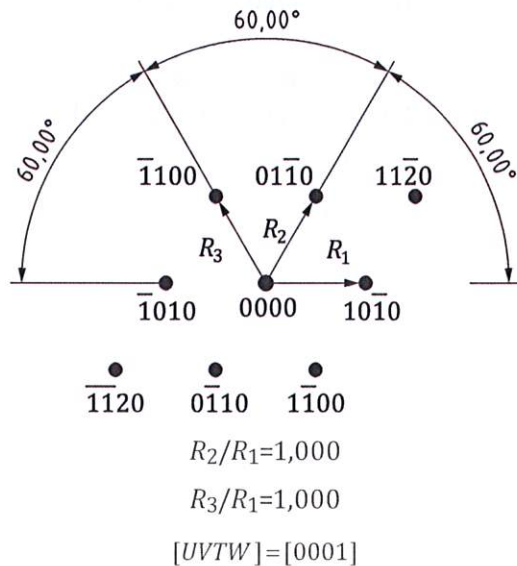
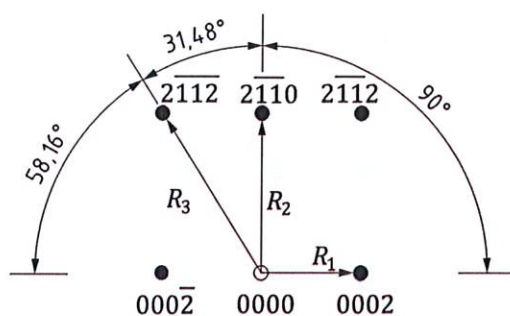


Figure B.31

ISO 25498:2018(E)



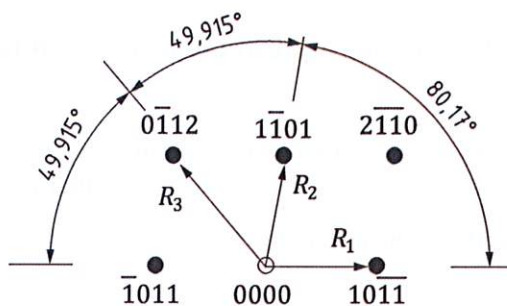
$\bar{2}11\bar{2}$ $\bar{2}110$ $\bar{2}112$

$R_2/R_1=1,633$

$R_3/R_1=1,915$

$[UVTW]=[01\bar{1}0]$

Figure B.32



$\bar{2}110$ $\bar{1}10\bar{1}$ $011\bar{2}$ $\times \bar{0}1\bar{2}\bar{3}$

$R_2/R_1=1,000$

$R_3/R_1=1,288$

$[UVTW]=[01\bar{1}1]$

Figure B.33

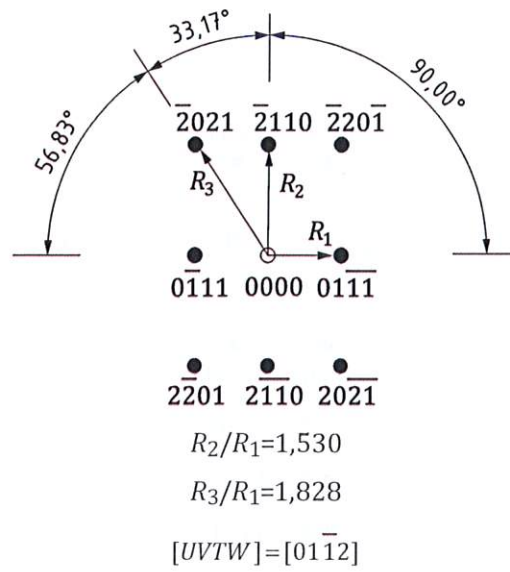


Figure B.34

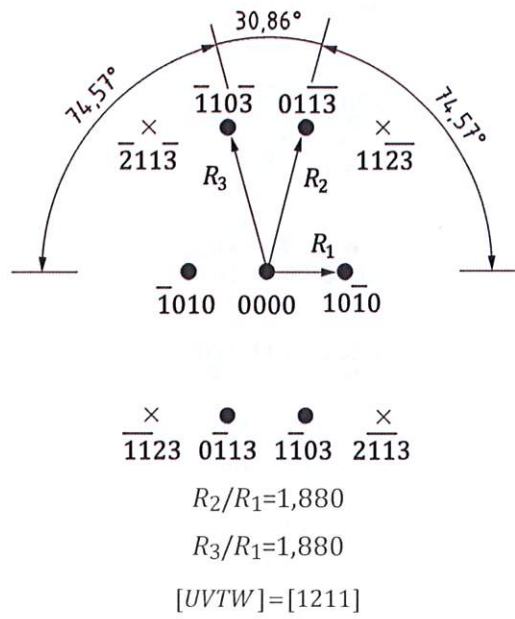


Figure B.35

ISO 25498:2018(E)

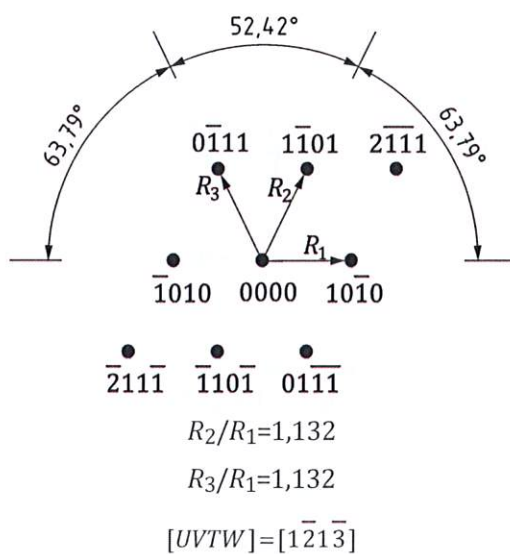


Figure B.36

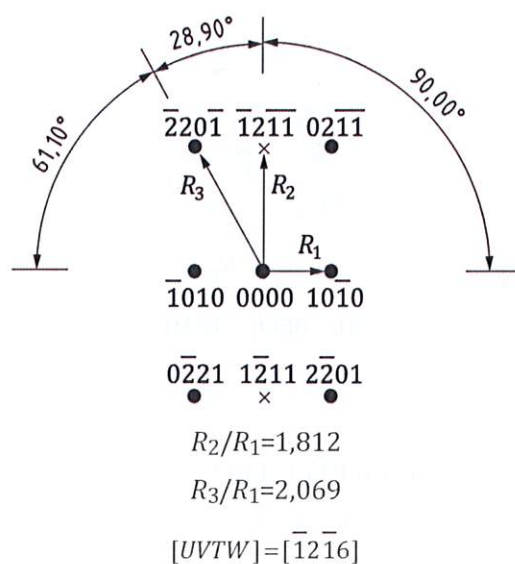
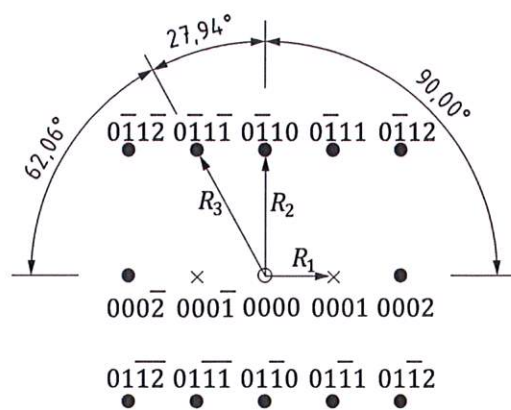


Figure B.37

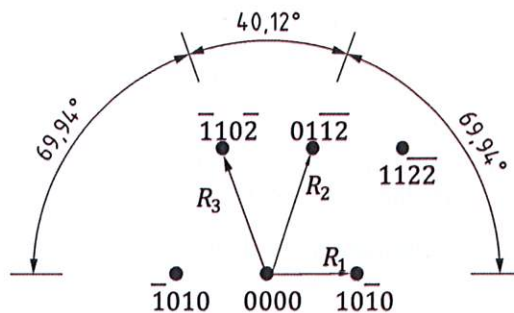


$$R_2/R_1=1,887$$

$$R_3/R_1=2,134$$

$$[UVTW]=[2\bar{1}10]$$

Figure B.38



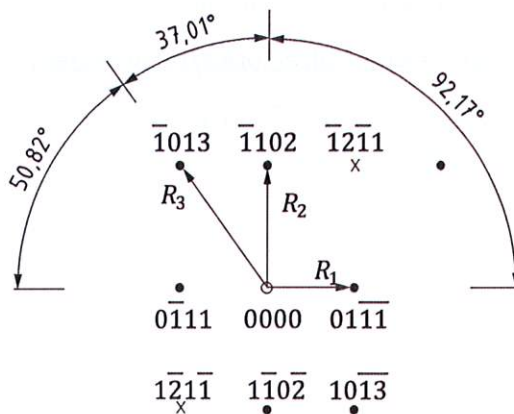
$$\begin{array}{ccc} \bullet & \bullet & \bullet \\ \hline 1122 & 0112 & 1102 \end{array}$$

$$R_2/R_1=1,458$$

$$R_3/R_1=1,458$$

$$[UVTW]=[\bar{2}4\bar{2}3]$$

Figure B.39



$$R_2/R_1=1,288$$

$$R_3/R_1=1,660$$

$$[UVTW]=[5\bar{1}43]$$

Figure B.40

ISO 25498:2018(E)

Bibliography

- [1] ISO 15932:2013, *Microbeam analysis — Analytical electron microscopy — Vocabulary*
- [2] ASTM E 3-11, Standard practice for preparation of metallographic specimens
- [3] Liu D.L., Features of the ISO-25498: Method of Selected Area Electron Diffraction Analysis in Transmission Electron Microscopy, *Microsc. Microanal.* 19, S5, 207–209, 2013
- [4] Williams, D.B. and Carter, C.B. *Transmission Electron Microscopy: A Textbook for Materials Science*, Plenum Press, New York 2009
- [5] Edington, J.W. *Practical Electron Microscopy in Materials Science, Vol. II, Electron Diffraction in The Electron Microscope*, Macmillan & Co Ltd, London, 1975
- [6] Guo, K.X., Ye, H.Q., Wu, Y.K., *Application of electron diffraction patterns in crystallography*, Science Press, China, 1983
- [7] Andrews, K.W., Dyson, D.J., Keown, S.R. *Interpretation of electron diffraction patterns*, Second Edition, 1971. (Publisher Hilger, London, ISBN-0-85274-170-7)
- [8] Reimer, L., *Transmission Electron Microscopy*, 4th Edition, Springer, 2004
- [9] Fultz, B, Howe, J., *Transmission Electron Microscopy and Diffractometry of Materials*, Springer-Verlag, Berlin Heidelberg 2001
- [10] Goodhew, P.J. *Specimen preparation for transmission electron microscopy of materials*, Oxford University Press, Royal Microscopical Society, 1984
- [11] The Powder Diffraction File 1997–2007, JCPDS, International Centre for Diffraction Data (ICDD)
- [12] Jiang, L, Georgieva, D., Zandbergen, H.W. and Abrahams, J.P. (2009) Unit-cell determination from randomly oriented electron-diffraction patterns. *Acta Cryst. D*, 625-632
- [13] <https://www.iucr.org/resources/other-directories/software/ediff>
- [14] Swanson, Tatge, *Natl. Bur. Stand. (US), Circ. 539*, 1, 11 (1953)

ISO 25498:2018(E)

ICS 71.040.50

Price based on 38 pages

© ISO 2018 - All rights reserved